Audio Engineering Society

Convention Paper 10510

Presented at the 151st Convention
2021 October, Online



# Audio-Source Rendering on Flat-Panel Loudspeakers with Non-Uniform Boundary Conditions

Michael C. Heilemann, Tre DiPassio, and Mark F. Bocko

*University of Rochester, Rochester, NY 14627, USA*

Correspondence should be addressed to Michael C. Heilemann (mheilema@ur.rochester.edu)

**ABSTRACT**

Devices from smartphones to televisions are beginning to employ dual purpose displays, where the display serves as both a video screen and a loudspeaker. In this paper we demonstrate a method to generate localized sound-radiating regions on a flat-panel display. An array of force actuators affixed to the back of the panel is driven by appropriately filtered audio signals so the total response of the panel due to the actuator array approximates a target spatial acceleration profile. The response of the panel to each actuator individually is initially measured via a laser vibrometer, and the required actuator filters for each source position are determined by an optimization procedure that minimizes the mean squared error between the reconstructed and targeted acceleration profiles. Since the single-actuator panel responses are determined empirically, the method does not require analytical or numerical models of the system's modal response, and thus is well-suited to panels having the complex boundary conditions typical of television screens, mobile devices, and tablets. The method is demonstrated on two panels with differing boundary conditions. When integrated with display technology, the localized audio source rendering method may transform traditional displays into multimodal audio-visual interfaces by colocating localized audio sources and objects in the video stream.

## 1 Introduction

Though flat-panel loudspeakers possess clear advantages over traditional cone loudspeakers in the areas of weight, form-factor, and the potential to serve as low-cost wave field synthesis arrays [1, 2], they have yet to experience any significant integration into commercial products. The development of the OLED display for smartphones, tablets, and televisions has sparked a renewed interest in flat-panel loudspeaker technology in the display industry [3, 4, 5]. One or more force actuators affixed to the back of an OLED display may be employed to induce bending motion in the panel, so that it radiates sound as a loudspeaker.

Recent studies on flat-panel loudspeakers demonstrated that actuator array-based excitation methods produce improved frequency response and directivity characteristics [6], as well as higher preference ratings in perceptual evaluations [7] when compared to single-actuator excitation methods [8, 9, 10]. A further advantage of array-based excitation methods is the potential to localize sound sources to a chosen region of the panel by designing filters based on the actuator position and the material properties of the panel, to control the magnitude and phase response of each actuator so that the net force on the panel excites a prescribed vibration profile [11]. On average, humans have a localization blur of 3.6° for sources in the forward direction according

to studies by [12] as presented in [13]. This implies even small, handheld devices subtend a large enough fraction of the viewing angle to provide spatial cues for localized audio sources rendered on the screen of the display and dynamically moved in real-time with spatially aligned images on the screen [14].

The filter parameters for the array-based excitation methods mentioned above are derived from theoretical models using ideal boundary conditions, which may not apply in practical settings such as display screens for tablets, televisions, and mobile devices, where the boundary conditions do not allow for a simple analytical representation of the modal response. One possible alternative is to derive the actuator filters from the empirically measured response of the panel. Li *et al*. [15] used a scanning laser vibrometer to obtain the vibration profile of the panel, and localize vibrations by designing filters to maximize the contrast in the kinetic energy between the vibrating region, and the non-vibrating region of the panel. While this method is effective at isolating vibrations to particular regions on the panel, the sound radiation qualities of these localized regions can exhibit irregularities in frequency response and directivity, as no specification is made regarding the vibration amplitude or spatial response within the vibrating region.

In this paper, a series of filters derived from empirical acceleration response measurements is applied to an array of actuators distributed on the surface of the panel to render localized sound sources. The magnitude and phase response of each actuator is determined by minimizing the mean squared error (MSE) between the reconstructed vibration profile of the panel and a specified target acceleration profile. Experiments on two panels with different boundary conditions demonstrate that this method may be used to localize sound-sources to specific regions of the panel below the spatial Nyquist frequency of the actuator array. This technique may be combined with existing methods of vibration localization to render sound sources for broadband object-based audio on displays [16].

## 2 Theoretical Development

The method for localizing sound-sources to specific vibrating regions of a panel is outlined in this section. In this analysis, the moving coil actuators are assumed to approximate point forces on the panel. Let a panel of surface area $S$, thickness $h$, and density $\rho$ have a complex spatial acceleration response $\tilde{\varphi}_i(x,y,\omega)$ when a complex excitation signal $\tilde{F}e^{j\omega t}$ is applied to an actuator located at position $(x_i,y_i)$.

Following Fuller [17] each spatial acceleration response is decomposed as a weighted superposition of resonant modes,

$$\tilde{\varphi}_i(x,y,\omega) = \sum_{r=1}^{\infty} -\omega^2 \tilde{F}\tilde{\alpha}_{ir}\Phi_r(x,y), \tag{1}$$

where $\Phi_r(x,y)$ is the spatial response of each resonant mode, and $\tilde{\alpha}_{ir}$ is the frequency dependent amplitude of each mode. As the boundary conditions of the system are unknown in the analysis, the spatial response of each mode may not be further specified. From [18], the amplitude of each mode may be expressed in terms of the actuator location, the resonant frequency of the mode $\omega_r$, and the quality factor of each mode $Q_r$ as,

$$\tilde{\alpha}_{ir} = \frac{4\Phi_r(x_i,y_i)}{\rho h S(\omega_r^2 - \omega^2 + j\omega_r\omega/Q_r)}. \tag{2}$$

The total response $\tilde{\varphi}(x,y,\omega)$ of a panel excited by an array of $N$ actuators, is given by the superposition of the responses to each actuator individually,

$$\tilde{\varphi}(x,y,\omega) = \sum_{i=1}^{N}\tilde{\varphi}_i(x,y,\omega) = \sum_{i=1}^{N}\sum_{r=1}^{\infty} -\omega^2\tilde{F}\tilde{\alpha}_{ir}\Phi_r(x,y), \tag{3}$$

The modal amplitudes $A_r$ of a specified target spatial acceleration profile $\Psi(x,y)$ may be determined by Fourier series expansion,

$$A_r = \frac{4}{S}\iint_S \Psi(x,y)\Phi_r(x,y)\,dy\,dx, \tag{4}$$

From (3) the total response of a panel excited by an array of $N$ actuators may be expressed as a sum of the modal excitations due to each actuator individually. A filter $\tilde{H}_i(\omega)$ with magnitude $|\tilde{H}_i(\omega)|$ and phase $\theta_i$ may be applied to the signal sent to each force actuator so that the weighted sum of the modal amplitudes of the panel's spatial acceleration profile match the modal amplitudes of $\Psi(x,y)$,

$$\sum_{i=1}^{N}\tilde{\alpha}_{ir}|\tilde{H}_i(\omega)|e^{j\theta_i} \approx A_r. \tag{5}$$

In reality, a finite number of $N$ actuators can physically be employed on the panel surface. This means that

the reconstruction of $\Psi(x,y)$ given in (5) is spatially band-limited to $N$ modes, and thus, some reconstructed mode amplitudes are an approximation of $A_r$.

Combining (3) and (5) gives the spatial response of the reconstructed acceleration profile.

$$\tilde{\varphi}(x,y,\omega) = \sum_{i=1}^{N}\sum_{r=1}^{\infty} -\omega^2 \tilde{F}\,\tilde{\alpha}_{ir}|\tilde{H}_i(\omega)|e^{j\theta_i}\Phi_r(x,y) = \sum_{i=1}^{N}\tilde{\varphi}_i(x,y,\omega)|\tilde{H}_i(\omega)|e^{j\theta_i}. \quad (6)$$

The filters for each actuator $\tilde{H}_i(\omega)$ are determined so that the MSE between the acceleration response magnitudes $|\tilde{\varphi}(x,y,\omega)|$ and $\Psi(x,y)$ is minimized for all frequencies. Each spatial response was discretized into $M$ subregions, each with area $\Delta x\Delta y$. The MSE is given by,

$$\text{MSE} = \frac{1}{M}\sum_{m=1}^{M}\left[|\tilde{\varphi}(x_m,y_m,\omega)| - \Psi(x_m,y_m)\right]^2. \quad (7)$$

where $\tilde{\varphi}(x_m,y_m,\omega)$ and $\Psi(x_m,y_m)$ are the accelerations of each response at the center of subregion $m$.

The approach follows some general techniques used for acoustic holography [19, 20, 21] and virtual speaker formation [22]. However, instead of inferring information about a sound source from a measured acoustic response, a specified vibration response is determined from a set of measured vibration responses. This allows for easy integration of visual/audio image pairing by directly controlling the vibrating surface itself. The reconstructed vibration response remains localized to a particular region of the panel where the in-phase motion of the vibrating region was shown to have uniform radiation properties below the spatial Nyquist frequency of the actuator array [23].

## 3 EXPERIMENTAL SETUP

The vibration localization method presented in the previous section was tested on two small panels with differing material properties and boundary conditions. The panels were made of 1 mm thick aluminum and 3 mm thick acrylic. Optimization of the panel materials and dimensions to maximize acoustic performance will be the subject of a different study. Both panels have dimensions $L_x = 113\,\text{mm}$, $L_y = 189\,\text{mm}$, and are excited by eight 3 W Dayton Audio DAEX13CT-8 audio exciters. The material properties of each panel are listed in Table 1.

**Table 1:** Young's Modulus $E$, density $\rho$, and Poisson's Ratio $\nu$ for various panel materials.

| Material | $E$ (GPa) | $\rho$ (kg m$^{-3}$) | $\nu$ | Supports |
|---|---|---|---|---|
| Aluminum | 68.9 | 2700 | 0.334 | Fixed Edges |
| Acrylic | 3.2 | 1180 | 0.35 | Standoffs |

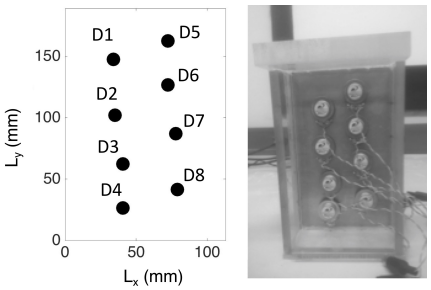


**Fig. 1:** Aluminum panel with fixed edges, and eight arbitrarily positioned actuators whose positions are indicated by black dots.

The aluminum panel was constructed to approximate clamped boundary conditions, where the spatial response of each mode is nearly sinusoidal [24]. The acrylic panel was supported by four standoffs, where each standoff is fixed approximately 2 cm in from each corner of the panel, and has a diameter of 1 cm. The boundary conditions in this case are not easily approximated analytically. The aluminum panel and the acrylic panel are shown with their corresponding actuator array layouts in Figs. 1 and 2 respectively.

### 3.1 Filter parameters

The vibration profile $\tilde{\varphi}_i(x,y)$ in response to excitation by each actuator individually was measured using a Polytec PSV-500 scanning laser vibrometer. The aluminum panel was measured over a frequency bandwidth of 4,000 Hz, to span the spatial Nyquist frequency of the driver array previously determined in [25]. The 2,000 Hz bandwidth used for the acrylic panel was determined empirically to span the spatial Nyquist frequency for the given driver array. Each actuator was powered by an independent Texas Instruments TPA3110D2 class-D amplifier channel.

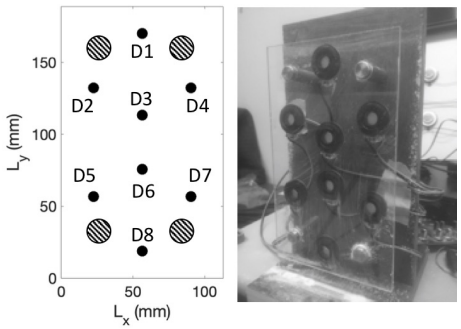


**Fig. 2:** Acrylic panel on four standoffs, with eight arbitrarily positioned actuators. The standoff and actuator positions are indicated by shaded circles, and black dots respectively.

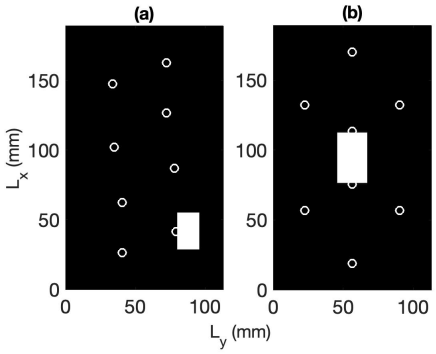


**Fig. 3:** Target acceleration profiles for the (a) aluminum and (b) acrylic panels. The actuator positions are indicated by white circles.

The target acceleration profiles for the panels are shown in Fig. 3. Each target acceleration profile is a rectangular region, where $\Psi(x,y)$ was given a normalized displacement value of unity inside the region, and zero outside the region. The target shape for the aluminum panel had dimensions $16.9\,\text{mm} \times 28.4\,\text{mm}$, and was centered at $(88.1\,\text{mm}, 43.5\,\text{mm})$. The target shape for the acrylic panel needed to be shifted in location to avoid overlapping one of the standoffs. The target shape for the acrylic panel had dimensions $L_x/5 \times L_y/5$, and the center point was the middle of the panel.

Following (7) the magnitudes and the phases of $\tilde{H}_i(\omega)$ needed to render the target acceleration profiles for the aluminum and acrylic panel is shown in Figs. 4 and 5 respectively, with $1/20^{\text{th}}$-octave smoothing. The magnitudes of the filters are presented in dB relative to

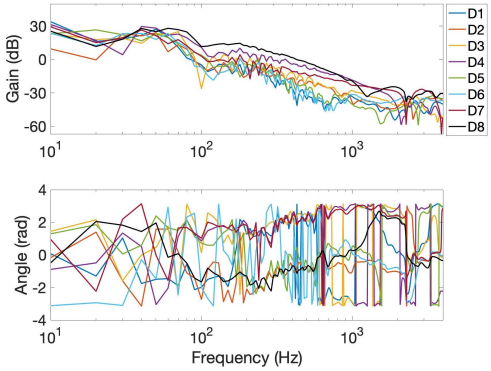


**Fig. 4:** Actuator filters for the aluminum panel shown in Fig 1 needed to render the target acceleration profile shown in 3a.

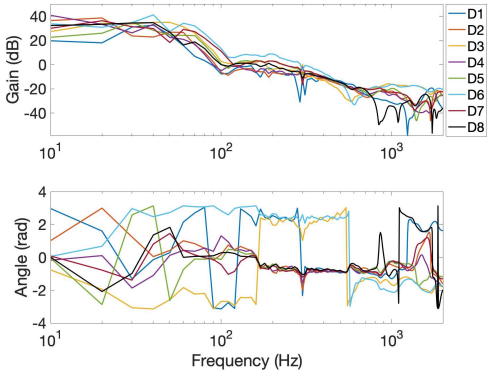


**Fig. 5:** Actuator filters for the acrylic panel shown in Fig 2 needed to render the target acceleration profile shown in 3b.

$1\,\text{m}\,\text{s}^{-2}$.

The filters resulting from the optimization exhibit an observable magnitude and phase variability at low frequency, as the optimization routine compensates for the high variability in $\tilde{\varphi}_i(x,y,\omega)$ due to the internal resonances of the actuators themselves, which couple the bending modes of the panel. The mass loaded resonances of these actuators is approximately 130 Hz. In practice, care may be taken when designing panels to ensure that the bending modes resonate above the resonant frequencies of the actuators to minimize actuator-mode coupling and reduce the effects of uncontrolled resonances [26].

The audio signal was filtered by $\tilde{H}_i(\omega)$ and sent to the respective actuators. The response of each panel was

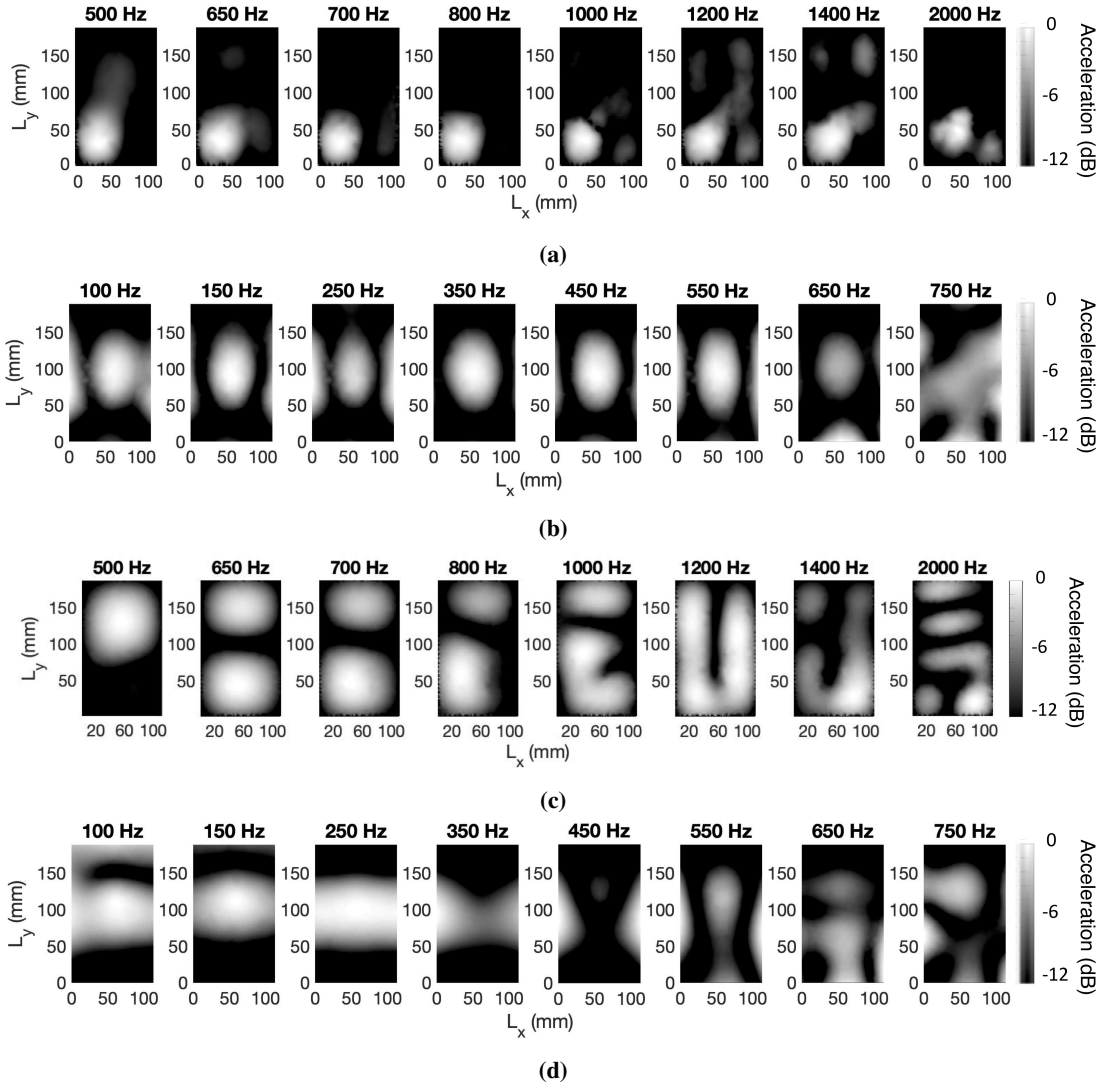


**Fig. 6:** Spatial acceleration response of the (a) aluminum, and (b) acrylic panels, where all actuators are weighted by the appropriate filter $\tilde{H}_i(\omega)$, and the spatial acceleration response of the (c) aluminum and (d) acrylic panel excited by the single actuator D3.

measured at different excitation frequencies using the scanning laser vibrometer. The acceleration responses of both panels are shown in Fig. 6 when all actuators are weighted by the specified filters $\tilde{H}_i(\omega)$. The acceleration responses of the panels are also shown for excitation by the single actuator D3 to demonstrate the natural response of the panel. The acceleration profiles are given in dB relative to the maximum acceleration at each frequency. Note that both panels were scanned from the front, so the source positions appear horizontally flipped compared to the targets. Since the aluminum panel has its lowest resonance at 401 Hz [11], the response of the panel is shown starting at 500 Hz to include frequencies where several different modes are excited.

For both the aluminum and acrylic panels, the rendered audio source remains localized to the intended region when excited at frequencies below the spatial Nyquist frequency of the array. It is important to note that the spatial Nyquist frequency of the actuator array places

a limit on the operational frequency bandwidth of this method. However, in an effect similar to the Schroeder frequency in room acoustics [27], vibrating panels undergo a transition in behavior from a low-frequency region where the response of the panel is dominated by individual modes, to a high-frequency region where the response of the panel remains localized around the driving element, and individual modal responses cannot be distinguished [28, 29]. While employing additional actuators can extend the addressable bandwidth of the actuator array and improve the resolution of the rendered target region, employing the array to localize vibrations above the panel's transition frequency can lead to diminishing returns as vibrations localize naturally at these frequencies due to the high modal overlap. Alternatively, a crossover network may be utilized to ensure that audio sources below the transition frequency are localized using the method described in the previous sections, while audio sources above the transition frequency are reproduced by a single actuator positioned near the intended source location.This will allow sources encoded in an object-based format such as MPEG-H 3D [30] to be rendered at their full bandwidth [16].

## 4 CONCLUSION

This paper describes methods that will enable the further development of spatial audio on flat-panel loudspeakers. Experiments employing the methods described here demonstrate that localized vibration regions may be rendered on the surface of a panel using filters designed using empirical measurements of the panel's vibration profile. This source rendering technique gives the potential to localize vibrations on the surfaces of displays such as laptop screens, televisions, and tablets, where the boundary conditions make the vibration profile of the system difficult to model in practice. These localized vibrations may serve as primary audio sources on the display screen and dynamically moved to new locations with their respective images, or held stationary on opposite sides of the panel to implement basic stereo imaging.

Much remains to be done in this area. Specifically, listening tests must be conducted to determine the perceptual effects of altering the size and shape of the different localized source regions. The results from these perceptual studies can help to determine an effective spatial resolution for vibrating regions, thus establishing a lower limit for the number of actuators required to render spatial audio on a given panel.

## 5 Acknowledgement

We gratefully acknowledge the support of NSF Award 2104758

## References

[1] Boone, M. M., "Multi-Actuator Panels (MAPs) as Loudspeaker Arrays for Wave Field Synthesis," *J. Audio Eng. Soc*, 52(7/8), pp. 712–723, 2004.

[2] Pueo, B., López, J. J., Escolano, J., and Hörchens, L., "Multiactuator panels for wave field synthesis: Evolution and present developments," *J. Audio Eng. Soc.*, 58(12), pp. 1045–1063, 2011.

[3] Lee, S., Park, K., Jang, K., and Oh, C., "Study on Enhancement of the Sound Quality by Improvement of Panel Vibration in OLED TV," in *SID Symposium Digest of Technical Papers*, volume 49, pp. 185–187, Wiley Online Library, 2018.

[4] Park, H., Park, S., and Bae, M.-J., "A Study on the Characteristics of Electroencephalography (EEG) by Listening Location of OLED Flat TV Speaker," in *International Conference on Computational Science/Intelligence & Applied Informatics*, pp. 83–92, Springer, 2018.

[5] Park, H. and Lee, S., "Analyzing Acoustic Characteristics of Multi-channel Speaker Directly Driving Flat Panel Display: Considering the Acoustic Stereo Effects," in *SID Symposium Digest of Technical Papers*, volume 50, pp. 1634–1636, Wiley Online Library, 2019.

[6] Anderson, D., Heilemann, M. C., and Bocko, M. F., "Impulse and Radiation Field Measurements for Single Exciter versus Exciter Array Flat-Panel Loudspeakers," in *Audio Engineering Society Convention 143*, Audio Engineering Society, 2017.

[7] Heilemann, M. C., Anderson, D., Roessner, S., and Bocko, M. F., "Quantifying Listener Preference of Flat-Panel Loudspeakers," in *Audio Engineering Society Convention 145*, Audio Engineering Society, 2018.

[8] Bank, G. and Harris, N., "The Distributed Mode Loudspeaker-Theory and Practice," in *AES 13th UK Conference: Microphones & Loudspeakers*, MAL-18, 1998.

[9] Gontcharov, V. P. and Hill, N. P. R., "Diffusivity Properties of Distributed Mode Loudspeakers," in *Audio Engineering Society Convention 108*, 5095, 2000.

[10] Zenker, B., Rawoof, S. S. A., Merchel, S., and Altinsoy, E., "Optimized Exciter Positioning Based on Acoustic Power of a Flat Panel Loudspeaker," in *Audio Engineering Society Convention 146*, Audio Engineering Society, 2019.

[11] Heilemann, M. C., Anderson, D., and Bocko, M. F., "Sound-Source Localization On Flat-Panel Loudspeakers," *J. Audio Eng. Soc*, 65(3), pp. 168–177, 2017.

[12] Preibisch-Effenberger, R., *The human faculty of sound localization and its audiometric application to clinical diagnostics*, Ph.D. thesis, Technische Universität, Dresden, 1966.

[13] Blauert, J., "Spatial hearing: the psychophysics of human sound source localization," 1983.

[14] Heilemann, M. C., Anderson, D., and Bocko, M. F., "Source rendering on dynamic audio displays," in *2017 IEEE Workshop on Applications of Signal Processing to Audio and Acoustics (WASPAA)*, pp. 334–338, IEEE, 2017.

[15] Li, Z., Luo, P., Zheng, C., and Li, X., "Vibrational Contrast Control for Local Sound Source Rendering on Flat Panel Loudspeakers," in *Audio Engineering Society Convention 145*, Audio Engineering Society, 2018.

[16] Heilemann, M. C., Anderson, D. A., and Bocko, M. F., "Near-Field Object-Based Audio Rendering on Flat-Panel Displays," *Journal of the Audio Engineering Society*, 67(7/8), pp. 531–539, 2019.

[17] Fuller, C., Elliott, S., and Nelson, P., *Active Control of Vibration*, Associated Press, 1996.

[18] Fahy, F. and Gardonio, P., *Sound and Structural Vibration: Radiation, Transmission and Response 2nd Edition*, Elsevier Science, 2007, ISBN 9780080471105.

[19] Williams, E. G., Maynard, J. D., and Skudrzyk, E., "Sound source reconstructions using a microphone array," *The Journal of the Acoustical Society of America*, 68(1), pp. 340–344, 1980, doi:10.1121/1.384602.

[20] Williams, E. G. and Maynard, J. D., "Holographic Imaging without the Wavelength Resolution Limit," *Phys. Rev. Lett.*, 45, pp. 554–557, 1980, doi:10.1103/PhysRevLett.45.554.

[21] Williams, E. G., Houston, B. H., and Bucaro, J. A., "Broadband nearfield acoustical holography for vibrating cylinders," *The Journal of the Acoustical Society of America*, 86(2), pp. 674–679, 1989, doi:10.1121/1.398245.

[22] Woo, J. and Ih, J., "Generation of a Virtual Speaker and Baffle on a Thin Plate Controlled by an Actuator Array at the Boundary," *IEEE/ASME Transactions on Mechatronics*, pp. 1–1, 2019, ISSN 1083-4435, doi:10.1109/TMECH.2019.2906376, early access.

[23] Heilemann, M. C., Anderson, D., and Bocko, M. F., "Equalization of Localized Sources on Flat-Panel Audio Displays," in *Audio Engineering Society Convention 143*, 2017.

[24] Mitchell, A. K. and Hazell, C. R., "A Simple Frequency Formula for Clamped Rectangular Plates," *J. Sound Vib.*, 118(2), pp. 271–281, 1987, doi:http://dx.doi.org/10.1016/0022-460X(87)90525-6.

[25] Anderson, D. A., Heilemann, M. C., and Bocko, M. F., "Optimized Driver Placement for Array-Driven Flat-Panel Loudspeakers," *Archives of Acoustics*, 42(1), pp. 93–104, 2017.

[26] Anderson, D. A., Heilemann, M. C., and Bocko, M. F., "Flat-Panel Loudspeaker Simulation Model with Electromagnetic Inertial Exciters and Enclosures," *J. Audio Eng. Soc.*, 65(9), pp. 722–732, 2017.

[27] Schroeder, M. R., "Statistical Parameters of the Frequency Response Curves of Large Rooms," *J. Audio Eng. Soc*, 35(5), pp. 299–306, 1987.

[28] Anderson, D. A., Heilemann, M. C., and Bocko, M. F., "Measures of vibrational localization on point-driven flat-panel loudspeakers," *Proceedings of Meetings on Acoustics*, 26(1), 2016, doi:http://dx.doi.org/10.1121/2.0000216.

[29] Rabbiolo, G., Bernhard, R., and Milner, F., "Definition of a high-frequency threshold for plates and acoustical spaces," *J. Sound Vib.*, 277(4–5), pp. 647 – 667, 2004, ISSN 0022-460X, doi: http://dx.doi.org/10.1016/j.jsv.2003.09.015.

[30] Herre, J., Hilpert, J., Kuntz, A., and Plogsties, J., "MPEG-H 3D Audio - The new standard for coding of immersive spatial audio," *IEEE Journal of selected topics in signal processing*, 9(5), pp. 770–779, 2015.